Non-linear stability analysis of a Darcy flow with viscous dissipation

***M. Celli[1], L. De B. Alves[2], A. Barletta[1]**

[1]Department of Industrial Engineering, Alma Mater Studiorum Università di Bologna,
Viale Risorgimento 2, 40136 Bologna, Italy

[2]Departamento de Engenharia Mecânica, Universidade Federal Fluminense,
Niterói, Rio de Janeiro, 24210-240, Brasil

*Corresponding author: michele.celli3@unibo.it

Abstract

The nonlinear convective instability of a flow in a fluid saturated impermeable and rectangular porous channel of arbitrary aspect ratio is here investigated by taking into account the effect of viscous dissipation. Darcy's law and Oberbeck-Boussinesq approximation are assumed. The vertical boundaries are assumed to be adiabatic and the horizontal boundaries are taken to be isothermal with the cold face placed on top. The system is characterised by two sources of thermal instability: the buoyancy activated by the non trivial temperature distribution due to the internal heat generation by the viscous dissipation and the buoyancy triggered by the non linear temperature distribution due to the temperature gap between the horizontal boundaries. The novel feature introduced in the present paper is the fully nonlinear approach to the stability analysis. The results obtained by the linear stability analysis are here used as a reference. The purpose of this paper is to analyse the system with the aim of finding possible subcritical instabilities. The technique employed in order to investigate the nonlinear problem is the generalized integral transform technique. The computational task relative to the integral transformation procedure and the solution of the ordinary differential equations obtained are carried out by *Mathematica 9* (© Wolfram Research).

Keywords: Nonlinear Stability, Generalised Integral Transform Technique, Porous Media, Viscous Dissipation, Thermal Convection

Introduction

The study of the onset of the thermal instabilities is an important topic with a deep engineering impact. In particular, the stability analyses of fluid saturated porous media have indeed several applications in a widespread range of scientific fields: from the oil extraction engineering to geological and geophysical studies and biological tissues convection heat and mass transfer. The source of thermal convection in fluid saturated porous media consists, typically, in the buoyancy force built up by heating from below boundary condition or an internal heat generation [Nield and Bejan (2013)]. In this paper, the buoyancy force is identified as the source of thermal instability and an internal generation effect, *viz.* the viscous dissipation, is employed in order to yield the buoyancy force. Analyses of this topic have been published by [Nield (2007)], [Storesletten and Barletta (2009)] and [Barletta, Celli and Rees (2009)]. The novel feature introduced in the present paper is the fully nonlinear approach to the stability analysis. The results obtained by the linear stability analysis are here used as a reference [Nield and Barletta (2010)]. In order to solve the nonlinear problem a specific mathematical technique is here employed: the generalized integral transform technique (GITT) [Cotta (1998)] and [Pontes, Alves and Cotta (2002)]. The GITT is an alternative hybrid numerical analytical technique based on the eigenfunction expansion in the spatial variables of the problem fields, *i.e.* velocity and temperature. The ordinary differential equations obtained by the integral transformation procedure constitute an initial value problem that is solved numerically. The computational task relative to the integral transformation procedure and the solution of the initial value problem are carried on by software that allow for mixed symbolic and numerical computations such as *Mathematica 9* (© Wolfram Research).

Mathematical model

A rectangular porous channel saturated by fluid with arbitrary aspect ratio is here investigated. A throughflow of give rate is assumed. The channel is considered impermeable while, for what concerns the thermal boundary conditions, the vertical channel walls are assumed to be adiabatic and the horizontal channel walls are assumed to be isothermal. A temperature gap, $\Delta T = T_h - T_c$, is imposed between the horizontal boundaries. The cold face, T_c, is placed on top and the hot face, T_h, is placed on the lower boundary. The Oberbeck-Boussinesq approximation is assumed, Darcy's law is employed in order to define the momentum balance equation and the viscous dissipation contribution inside the energy balance equation is taken into account as internal heat source. The curl operator is applied to Darcy's law so that the governing equations lose the pressure gradient contribution. The dimensionless governing equations that describe the system together with the relative boundary conditions are

$$\begin{aligned}
&\boldsymbol{\nabla}\cdot\boldsymbol{u} = 0,\\
&\boldsymbol{\nabla}\times\boldsymbol{u} = \boldsymbol{\nabla}\times(T\boldsymbol{e}_y),\\
&\frac{\partial T}{\partial t} + \boldsymbol{u}\cdot\boldsymbol{\nabla}T = \nabla^2 T + Ge\,\boldsymbol{u}\cdot\boldsymbol{u},\\
&x = 0, s: \qquad u = 0, \qquad \frac{\partial T}{\partial x} = 0,\\
&y = 0, 1: \qquad v = 0, \qquad T = R, 0.
\end{aligned} \tag{1}$$

where $\boldsymbol{u} = (u, v, w)$ is the velocity vector, T is the temperature, $\boldsymbol{e}_y$ is the unit vector of the y-axis, t is the time, Ge the Gebhart number, R the Rayleigh number and s is the aspect ratio. A sketch of the geometry and a description of the boundary conditions is reported in Fig. 1. The scaling employed in order to obtain the dimensionless formulation is the following

$$\begin{gathered}
\bar{t} = \frac{\sigma H^2}{\alpha} t, \quad \bar{\boldsymbol{x}} = H\boldsymbol{x}, \quad \bar{\boldsymbol{u}} = \frac{\alpha}{H}\boldsymbol{u}, \quad \overline{T} = T_c + \Delta T \frac{T}{R},\\
Ge = \frac{g\beta H}{c}, \quad R = \frac{g\beta\Delta T H K}{\nu\alpha}, \quad s = \frac{L}{H},
\end{gathered} \tag{2}$$

where the dimensional quantities are over-lined, σ is the dimensionless ratio between the average heat capacity per unit volume of the porous medium and the average heat capacity per unit volume of the fluid, H is the height of the channel, α is the effective thermal diffusivity, ν is the kinematic viscosity, K is the permeability, c is the specific heat, g is the modulus of gravity acceleration, β is the thermal expansion coefficient and L is the width of the channel.

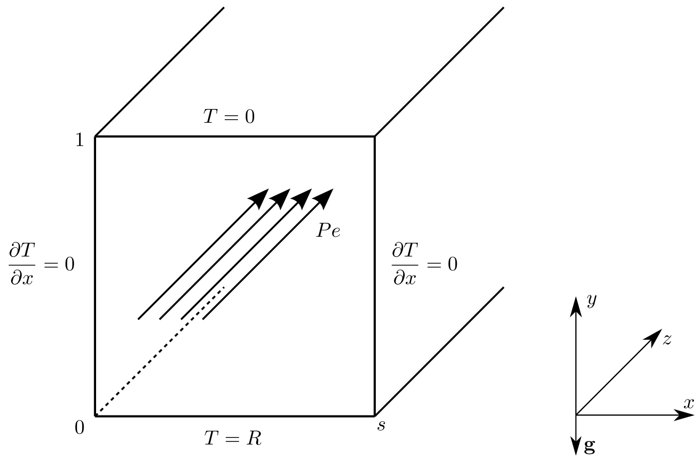

Figure 1. A sketch of the porous channel and its boundary conditions

Basic stationary solution

The first step in this stability analysis consists in redefining the velocity and temperature fields as composed by two contributions: a stationary basic state and a perturbed field, namely

$$\boldsymbol{u} = \boldsymbol{u}_b + \boldsymbol{U}, \quad T = T_b + \Theta, \tag{3}$$

where the subscript b refers to the basic state. In the following we will need also the initial values of velocity and temperature perturbed fields. These initial values are defined as a combination of an initial value of the perturbed field plus the basic stationary flow contribution.

$$t = 0: \qquad \boldsymbol{u} = \boldsymbol{u}_b + \boldsymbol{U}_0, \quad T = T_b + \Theta_0. \tag{4}$$

The stability analysis is here performed with respect to a particular stationary solution of the governing equations (1). A constant throughflow in the z-direction is assumed and the temperature field of this fully developed flow is assumed to be dependent only on the y-coordinate, namely

$$\boldsymbol{u}_b = \{0, 0, Pe\}, \quad T_b = \frac{(1-y)(2R + \Lambda y)}{2}. \tag{5}$$

The Péclet number is defined through the average velocity over the channel, $Pe = w_b L/\alpha$, and the parameter $\Lambda = Ge\, Pe^2$. Inside the setup just described we may identify two possible mechanisms capable to generate thermal instabilities: the coupling between the buoyancy force and the heat generated by viscous dissipation and the coupling between the buoyancy force and the vertical temperature gradient produced by ΔT. Each mechanism is regulated by means of a nondimensional parameter: Λ regulates the strength of the buoyancy force due to the viscous dissipation contribution whereas R regulates the strength of the buoyancy force due to Darcy-Bènard-like mechanism coming from the temperature gap ΔT.

Perturbed equations

On applying the Eq. (3) to Eq. (1) and subtracting the basic stationary state contribution one obtains

$$\begin{gathered} \boldsymbol{\nabla} \cdot \boldsymbol{U} = 0, \\ \boldsymbol{\nabla} \times \boldsymbol{U} = \boldsymbol{\nabla} \times (\Theta \boldsymbol{e}_y), \\ \frac{\partial \Theta}{\partial t} + V \frac{\partial T_b}{\partial y} + Pe \frac{\partial \Theta}{\partial z} + \boldsymbol{U} \cdot \boldsymbol{\nabla} \Theta = \nabla^2 \Theta + 2\, Ge\, Pe\, W + Ge\, \boldsymbol{U} \cdot \boldsymbol{U}. \end{gathered} \tag{6}$$

The investigation may now be reduced in complexity by focusing our attention only on the longitudinal rolls and disregarding the other possible inclinations of the disturbances. Since the longitudinal rolls lie on the (x,y)-plane, the contributions of those term in the equations that refer to the z-direction are thus neglected. On introducing the streamfunction $U = \partial\Psi/\partial y$ and $V = -\partial\Psi/\partial x$, the governing equations (6), the relative boundary conditions and the initial values reduce to

$$\nabla^2\Psi = -\frac{\partial\Theta}{\partial x}, \tag{7a}$$

$$\frac{\partial\Theta}{\partial t} - \frac{\partial T_b}{\partial y}\frac{\partial\Psi}{\partial x} + \frac{\partial\Psi}{\partial y}\frac{\partial\Theta}{\partial x} - \frac{\partial\Psi}{\partial x}\frac{\partial\Theta}{\partial y} = \frac{\partial^2\Theta}{\partial x^2} + \frac{\partial^2\Theta}{\partial y^2} + Ge\left(\frac{\partial\Psi}{\partial y}\right)^2 + Ge\left(\frac{\partial\Psi}{\partial x}\right)^2, \tag{7b}$$

$$\begin{aligned} &x = 0, s: && \Psi = 0, && \frac{\partial\Theta}{\partial x} = 0,\\ &y = 0, 1: && \Psi = 0, && \Theta = 0,\\ &t = 0: && \Psi = \Psi_0(x,y), && \Theta = \Theta_0(x,y). \end{aligned} \tag{7c}$$

Since Eq. (7a) does not show a time dependency, the initial value for the streamfunction filed is not necessary. On the other hand, the shape of Θ_0 is chosen to be equal to the temperature field configuration of a single longitudinal roll occupying the whole channel, $\Theta_0(x,y) = \cos(\pi x/s)\sin(\pi y)$. One may note that the value of the perturbation amplitude for Θ_0 is of $O(1)$. The choice of this order of magnitude comes from the necessity to distinguish this analysis from the linear stability one. The linear stability analysis requires, indeed, to employ perturbations small enough so that the nonlinear terms in the perturbations inside the governing equations may be neglected.

The Generalised Integral Transform Technique

In order to perform the nonlinear stability analysis the Generalised Integral Transform Technique (GITT) is employed. The GITT starts with the eigenfunction expansion of the problem potential on the spatial variables. For what concerns the streamfunction field, the so-called auxiliary eigenvalue problems in the x and y-directions are

$$\frac{\mathrm{d}^2\bar{\psi}_i(x)}{\mathrm{d}x^2} + \lambda_i^2\bar{\psi}_i(x) = 0, \qquad \bar{\psi}_i(0) = \bar{\psi}_i(s) = 0, \tag{8a}$$

$$\frac{\mathrm{d}^2\tilde{\psi}_j(y)}{\mathrm{d}y^2} + \omega_j^2\tilde{\psi}_j(y) = 0, \qquad \tilde{\psi}_j(0) = \tilde{\psi}_j(1) = 0. \tag{8b}$$

The relative eigenfunctions and eigenvalues are

$$\bar{\psi}_i(x) = \sqrt{\frac{2}{s}}\sin(\lambda_i x), \quad \lambda_i = \frac{i\pi}{s}, \quad i = 1, 2, ... \tag{9a}$$

$$\tilde{\psi}_j(y) = \sqrt{2}\sin(\omega_j y), \quad \omega_j = j\pi, \quad j = 1, 2, ... \tag{9b}$$

For what concerns the temperature field, the so-called auxiliary eigenvalue problems in the x and y-directions are

$$\frac{\mathrm{d}^2\bar{\theta}_m(x)}{\mathrm{d}x^2} + \gamma_m^2\bar{\theta}_m(x) = 0, \qquad \frac{\mathrm{d}\bar{\theta}_m(0)}{\mathrm{d}x} = \frac{\mathrm{d}\bar{\theta}_m(s)}{\mathrm{d}x} = 0, \tag{10a}$$

$$\frac{\mathrm{d}^2\tilde{\theta}_n(y)}{\mathrm{d}y^2} + \sigma_n^2\tilde{\theta}_n(y) = 0, \qquad \bar{\theta}_n(0) = \bar{\theta}_n(1) = 0. \tag{10b}$$

The relative eigenfunctions and eigenvalues are

$$\bar{\theta}_0(x) = \frac{1}{s}, \quad \bar{\theta}_m(x) = \sqrt{\frac{2}{s}}\cos(\gamma_m x), \quad \gamma_m = \frac{m\pi}{s}, \quad m = 1,2,... \tag{11a}$$

$$\tilde{\theta}_n(y) = \sqrt{2}\sin(\sigma_n y), \quad \sigma_n = n\pi, \quad n = 1,2,...,. \tag{11b}$$

The GITT is based on the expansion of Eq. (7) by means of the eigenfuctions and eigenvalues Eqs. (9) and Eqs. (11). The next step in the solution procedure consists in integral transforming Eq. (7). The streamfunction transform relations pair, and the relative inverse relations, are defined as follows

$$\begin{aligned} \bar{\Psi}_i(y,t) &= \int_0^s \bar{\psi}_i(x)\Psi(x,y,t)\mathrm{d}x, \qquad \Psi(x,y,t) = \sum_{i=1}^{\infty} \bar{\psi}_i(x)\bar{\Psi}_i(y,t), \\ \tilde{\bar{\Psi}}_{i,j}(t) &= \int_0^1 \tilde{\psi}_j(y)\bar{\Psi}_i(y,t)\mathrm{d}y, \qquad \bar{\Psi}_i(y,t) = \sum_{j=1}^{\infty} \tilde{\psi}_j(y)\tilde{\bar{\Psi}}_{i,j}(t). \end{aligned} \tag{12}$$

The temperature transform relations pair, and the relative inverse relations, are

$$\begin{aligned} \bar{\Theta}_m(y,t) &= \int_0^s \bar{\theta}_m(x)\Theta(x,y,t)\mathrm{d}x, \qquad \Theta(x,y,t) = \sum_{m=0}^{\infty} \bar{\theta}_m(x)\bar{\Theta}_m(y,t), \\ \tilde{\bar{\Theta}}_{m,n}(t) &= \int_0^1 \tilde{\theta}_n(y)\bar{\Theta}_m(y,t)\mathrm{d}y, \qquad \bar{\Theta}_m(y,t) = \sum_{n=1}^{\infty} \tilde{\theta}_n(y)\tilde{\bar{\Theta}}_{m,n}(t). \end{aligned} \tag{13}$$

Integral transform procedure

In order to perform the integral transformation of Eq. (7), we start working on the streamfunction equation. We first multiply Eq. (7a) by the eigenfunction of the auxiliary problem for the streamfunction in the x-direction $\bar{\psi}_i(x)$ of Eqs. (9a) and then we integrate over x to obtain

$$\int_0^s \bar{\psi}_i(x)\left[\frac{\partial^2\Psi(x,y,t)}{\partial x^2} + \frac{\partial^2\Psi(x,y,t)}{\partial y^2}\right]\mathrm{d}x = -\int_0^s \bar{\psi}_i(x)\frac{\partial\Theta(x,y,t)}{\partial x}\mathrm{d}x. \tag{14}$$

Equation (14) can be integrated by applying the integration by parts, by applying the boundary conditions in Eqs. (7c) and by applying the inverse definition in Eqs. (12). The integration yield to the following expression

$$\frac{\partial^2\bar{\Psi}_i(y,t)}{\partial y^2} - \lambda_i^2\bar{\Psi}_i(y,t) = -\sum_{m=0}^{\infty}\bar{A}_{i,m}\bar{\Theta}_m(y,t), \tag{15}$$

With the integral transform coefficient $A_{i,m}$ defined as

$$\bar{A}_{i,m} = \int_0^s \bar{\psi}_i(x)\frac{\mathrm{d}\bar{\theta}_m(x)}{\mathrm{d}x}\mathrm{d}x \tag{16}$$

We thus multiply Eq. (15) by the eigenfunction of the auxiliary problem for the streamfunction in the y-direction $\tilde{\psi}_j(y)$ of Eqs. (9b) and then we integrate over y to obtain

$$\int_0^1 \tilde{\psi}_j(y)\frac{\partial^2\bar{\Psi}_i(y,t)}{\partial y^2}\mathrm{d}y - \lambda_i^2\int_0^1 \tilde{\psi}_j(y)\bar{\Psi}_i(y,t)\mathrm{d}y = -\sum_{m=0}^{\infty}\bar{A}_{i,m}\int_0^1 \tilde{\psi}_j(y)\bar{\Theta}_m(y,t)\mathrm{d}y. \tag{17}$$

On following the same procedure employed to obtain Eq. (15) one can write

$$(\lambda_i^2+\omega_j^2)\tilde{\bar{\Psi}}_{i,j}(t)=\sum_{m=0}^{\infty}\sum_{n=0}^{\infty}A_{i,j,m,n}\tilde{\bar{\Theta}}_{m,n}(t), \tag{18}$$

where the integral transform coefficient $A_{i,j,m,n}$

$$A_{i,j,m,n}=\bar{A}_{i,m}\tilde{A}_{j,n}\,,\qquad \tilde{A}_{j,n}=\int_0^1\tilde{\psi}_j(y)\tilde{\theta}_n(y)\mathrm{d}y \tag{19}$$

We may now start transforming the equation for the perturbed temperature. We thus multiply Eq. (7b) by the eigenfunction of the auxiliary problem for the temperature in the x-direction $\bar{\theta}_m(x)$ of Eqs. (10a) and then we integrate over x to obtain

$$\begin{aligned}
&\int_0^s\frac{\partial\Theta(x,y,t)}{\partial t}\bar{\theta}_m(x)\mathrm{d}x-\frac{\partial T_b}{\partial y}\int_0^s\frac{\partial\Psi(x,y,t)}{\partial x}\bar{\theta}_m(x)\mathrm{d}x+\int_0^s\frac{\partial\Psi(x,y,t)}{\partial y}\frac{\partial\Theta(x,y,t)}{\partial x}\bar{\theta}_m(x)\mathrm{d}x\\
&-\int_0^s\frac{\partial\Psi(x,y,t)}{\partial x}\frac{\partial\Theta(x,y,t)}{\partial y}\bar{\theta}_m(x)\mathrm{d}x=\int_0^s\frac{\partial^2\Theta(x,y,t)}{\partial x^2}\bar{\theta}_m(x)\mathrm{d}x+\int_0^s\frac{\partial^2\Theta(x,y,t)}{\partial y^2}\bar{\theta}_m(x)\mathrm{d}x\\
&+Ge\int_0^s\left(\frac{\partial\Psi(x,y,t)}{\partial y}\right)^2\bar{\theta}_m(x)\mathrm{d}x+Ge\int_0^s\left(\frac{\partial\Psi(x,y,t)}{\partial x}\right)^2\bar{\theta}_m(x)\mathrm{d}x.
\end{aligned} \tag{20}$$

The integration of Eq. (20) is based on the same procedure employed for the streamfunction thus using the relations in Eqs. (11) and (12) and the integration by parts. The following equation is obtained

$$\begin{aligned}
&\frac{\partial\bar{\Theta}_m(y,t)}{\partial t}-\frac{\partial T_b}{\partial y}\sum_{i=1}^{\infty}\bar{B}_{m,i}\bar{\Psi}_i(y,t)+\sum_{i=1}^{\infty}\sum_{o=0}^{\infty}\bar{C}_{m,i,o}\frac{\partial\bar{\Psi}_i(y,t)}{\partial y}\bar{\Theta}_o(y,t)\\
&-\sum_{i=1}^{\infty}\sum_{o=0}^{\infty}\bar{D}_{m,i,o}\frac{\partial\bar{\Theta}_o(y,t)}{\partial y}\bar{\Psi}_i(y,t)=-\gamma_m^2\bar{\Theta}_m(y,t)\\
&+Ge\left[\sum_{i=1}^{\infty}\sum_{o=1}^{\infty}\bar{E}_{m,i,o}\frac{\partial\bar{\Psi}_i(y,t)}{\partial y}\frac{\partial\bar{\Psi}_o(y,t)}{\partial y}+\sum_{i=1}^{\infty}\sum_{o=1}^{\infty}\bar{F}_{m,i,o}\bar{\Psi}_i(y,t)\bar{\Psi}_o(y,t)\right],
\end{aligned} \tag{21}$$

where the integral transform coefficients are defined as

$$\begin{aligned}
&\bar{B}_{m,i}=\int_0^s\frac{\mathrm{d}\bar{\psi}_i(x)}{\mathrm{d}x}\bar{\theta}_m(x)\mathrm{d}x,\quad \bar{C}_{m,i,o}=\int_0^s\bar{\psi}_i(x)\frac{\mathrm{d}\bar{\theta}_o(x)}{\mathrm{d}x}\bar{\theta}_m(x)\mathrm{d}x,\\
&\bar{D}_{m,i,o}=\int_0^s\frac{\mathrm{d}\bar{\psi}_i(x)}{\mathrm{d}x}\bar{\theta}_o(x)\bar{\theta}_m(x)\mathrm{d}x,\quad \bar{E}_{m,i,o}=\int_0^s\bar{\psi}_i(x)\bar{\psi}_o(x)\bar{\theta}_m(x)\mathrm{d}x,\\
&\bar{F}_{m,i,o}=\int_0^s\frac{\mathrm{d}\bar{\psi}_i(x)}{\mathrm{d}x}\frac{\mathrm{d}\bar{\psi}_o(x)}{\mathrm{d}x}\bar{\theta}_m(x)\mathrm{d}x.
\end{aligned} \tag{22}$$

We can now proceed multiplying Eq. (21) by the eigenfunction of the auxiliary problem for the temperature in the y-direction $\tilde{\theta}_n(y)$ of Eqs. (10b) and then integrating over y

$$\begin{aligned}
&\int_0^1\tilde{\theta}_n(y)\frac{\partial\bar{\Theta}_m(y,t)}{\partial t}\mathrm{d}y-\int_0^1\tilde{\theta}_n(y)\frac{\partial T_b}{\partial y}\sum_{i=1}^{\infty}B_{m,i}\bar{\Psi}_i(y,t)\mathrm{d}y\\
&+\int_0^1\tilde{\theta}_n(y)\sum_{i=1}^{\infty}\sum_{o=0}^{\infty}C_{m,i,o}\frac{\partial\bar{\Psi}_i(y,t)}{\partial y}\bar{\Theta}_o(y,t)\mathrm{d}y-\int_0^1\tilde{\theta}_n(y)\sum_{i=1}^{\infty}\sum_{o=0}^{\infty}D_{m,i,o}\frac{\partial\bar{\Theta}_o(y,t)}{\partial y}\bar{\Psi}_i(y,t)\mathrm{d}y\\
&=-\int_0^1\tilde{\theta}_n(y)\gamma_m^2\bar{\Theta}_m(y,t)\mathrm{d}y+\int_0^1\tilde{\theta}_n(y)\frac{\partial^2\bar{\Theta}_m(y,t)}{\partial y^2}\mathrm{d}y\\
&+Ge\int_0^1\tilde{\theta}_n(y)\left[\sum_{i=1}^{\infty}\sum_{o=1}^{\infty}E_{m,i,o}\frac{\partial\bar{\Psi}_i(y,t)}{\partial y}\frac{\partial\bar{\Psi}_o(y,t)}{\partial y}+\sum_{i=1}^{\infty}\sum_{o=1}^{\infty}F_{m,i,o}\bar{\Psi}_i(y,t)\bar{\Psi}_o(y,t)\right]\mathrm{d}y.
\end{aligned} \tag{23}$$

What is obtained integrating Eq. (23) with the technique employed for Eq. (21) is

$$\begin{aligned}
&\frac{d\tilde{\bar{\Theta}}_{m,n}(t)}{dt}-\sum_{i=1}^{\infty}\sum_{j=1}^{\infty}B_{m,n,i,j}\tilde{\bar{\Psi}}_{i,j}(t)+\sum_{i=1}^{\infty}\sum_{j=1}^{\infty}\sum_{o=0}^{\infty}\sum_{p=0}^{\infty}\left(C_{m,n,i,j,o,p}-D_{m,n,i,j,o,p}\right)\tilde{\bar{\Psi}}_{i,j}(t)\tilde{\bar{\Theta}}_{o,p}(t)\\
&\quad=-(\gamma_m^2+\sigma_n^2)\tilde{\bar{\Theta}}_{m,n}(t)+Ge\sum_{i=1}^{\infty}\sum_{j=1}^{\infty}\sum_{o=1}^{\infty}\sum_{p=1}^{\infty}\left(E_{m,n,i,j,o,p}+F_{m,n,i,j,o,p}\right)\tilde{\bar{\Psi}}_{i,j}(t)\tilde{\bar{\Psi}}_{o,p}(t),
\end{aligned}\tag{24}$$

where the integral transform coefficients are defined as

$$\begin{aligned}
B_{m,n,i,j}&=\bar{B}_{m,i}\tilde{B}_{n,j}=\bar{B}_{m,i}\int_0^1\frac{\partial T_b}{\partial y}\tilde{\psi}_j(y)\,\tilde{\theta}_n(y)\mathrm{d}y,\\
C_{m,n,i,j,o,p}&=\bar{C}_{m,i,o}\tilde{C}_{n,j,p}=\bar{C}_{m,i,o}\int_0^1\frac{\mathrm{d}\tilde{\psi}_j(y)}{\mathrm{d}y}\tilde{\theta}_p(y)\tilde{\theta}_n(y)\mathrm{d}y,\\
D_{m,n,i,j,o,p}&=\bar{D}_{m,i,o}\tilde{D}_{n,j,p}=\bar{D}_{m,i,o}\int_0^1\tilde{\psi}_j(y)\frac{\mathrm{d}\tilde{\theta}_p(y)}{\mathrm{d}y}\tilde{\theta}_n(y)\mathrm{d}y,\\
E_{m,n,i,j,o,p}&=\bar{E}_{m,i,o}\tilde{E}_{n,j,p}=\bar{E}_{m,i,o}\int_0^1\frac{\mathrm{d}\tilde{\psi}_j(y)}{\mathrm{d}y}\frac{\mathrm{d}\tilde{\psi}_p(y)}{\mathrm{d}y}\tilde{\theta}_n(y)\mathrm{d}y,\\
F_{m,n,i,j,o,p}&=\bar{F}_{m,i,o}\tilde{F}_{n,j,p}=\bar{F}_{m,i,o}\int_0^1\tilde{\psi}_j(y)\,\tilde{\psi}_p(y)\tilde{\theta}_n(y)\mathrm{d}y.
\end{aligned}\tag{25}$$

In order to complete the initial value problem, we now integral transform the perturbed contribution of the initial values in Eqs. (4), namely

$$\tilde{\bar{\Psi}}_{i,j}(0)=f_{i,j},\quad \tilde{\bar{\Theta}}_{m,n}(0)=g_{m,n},\tag{26}$$

where

$$\begin{aligned}
f_{i,j}&=\int_0^s\bar{\psi}_i(x)\,\mathrm{d}x\int_0^1\tilde{\psi}_j(y)\,\Psi_0(x,y)\,\mathrm{d}y,\\
g_{m,n}&=\int_0^s\bar{\theta}_m(x)\,\mathrm{d}x\int_0^1\tilde{\theta}_n(y)\,\Theta_0(x,y)\,\mathrm{d}y.
\end{aligned}\tag{27}$$

Discussion of the results and concluding remarks

The task of this investigation is comparing the results obtained by the nonlinear analysis with the values obtained by the linear stability analysis. We start switching off the contribution of the Darcy-Bènard-like instability source: whenever the temperature gap between the horizontal boundaries is negligible, *viz.* $R=0$, the relative buoyancy force contribution is absent. With $R=0$ the linear stability analysis responds a threshold value for the governing parameter $\Lambda_{cr}=471.38$ and a threshold value for the wavenumber $k_{cr}=4.6752$, [Nield and Barletta (2010)]. The subscript cr stands for critical value. Figures (2) and (3) show the neutral stability curves obtained fixing $R=0$ for different values of Ge as functions of the aspect ratio s. The different curves reported in the frames refer to different values of the number of equations employed to model the problem. The eigenfunction expansion has, in fact, to be truncated at some point and n is the number of equations obtained with the different choices of the truncation point. In Fig. 2 and Fig. 3 the dotted lines refer to those truncation points that produce a number of equations $n=30$, the dashed lines refer to $n=60$ and the continuous lines to $n=90$. Figures (2) and (3) prove that the present nonlinear analysis reproduce exactly the same minimum (highlighted by the horizontal dashed line $\Lambda_{cr}=471.38$) obtained by the linear stability analysis. The value of the aspect ratio, relative to second minimum of Λ, results to be equal to the wavelength corresponding to the critical wavenumber value $k_{cr}=4.6752$ obtained by the linear stability analysis. The difference between Fig. 2 and Fig. 3 lies on the values of the Gebhart number

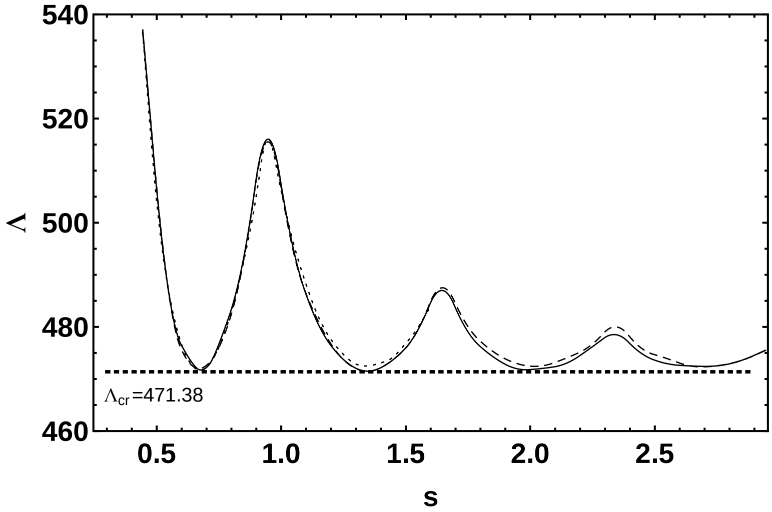

Figure 2. Critical values of Λ as a function of the aspect ratio s for $Ge \to 0$, $R = 0$ and different values of the number of equations employed n

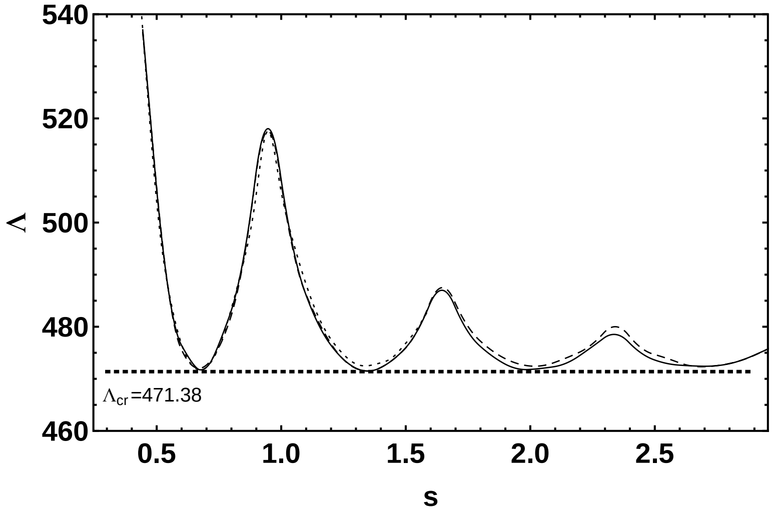

Figure 3. Critical values of Λ as a function of the aspect ratio s for $Ge = 1$, $R = 0$ and different values of the number of equations employed n

assumed: Fig. 2 refers to $Ge \to 0$ and Fig. 3 is refers to $Ge = 1$. The limit $Ge \to 0$ is compatible with finite values of Λ if we consider, together with the limit $Ge \to 0$, a fast basic flow, *viz.* $Pe \gg 1$. Figure (4) shows a comparison between the neutral stability curves obtained with $R = 0$, $n = 90$ and two different values of the Gebhart number: $Ge \to 0$, the continuous line, and $Ge = 1$, the dashed line. This figure shows how the system results not to be sensitive to the magnitude of the Gebhart number. We proceed switching off the viscous dissipation and looking for the Darcy-Bénard-like instability. In order to neglect the viscous dissipation contribution the limits $Ge \to 0$ and $\Lambda \to 0$ are considered. In this case the linear stability analysis responds a threshold value for the critical parameter $R_{cr} = 4\pi^2$ and a wavenumber $k_{cr} = \pi$, [Nield and Barletta (2010)]. Figure (5) shows the neutral stability curves for $Ge \to 0$ and $\Lambda = 10^{-4}$. Once again the dotted line refer to those truncation points that produce a number of equations $n = 30$, the dashed line refer to $n = 60$ and the continuous line to $n = 90$. These curves show that the present nonlinear analysis reproduces exactly the same minimum (highlighted by the horizontal dashed line $R_{cr} = 4\pi^2$) found by the linear stability analysis. Moreover, the critical aspect ratio value relative to the second minimum in Fig. 5 is equals to the wavelength corresponding to the critical wavenumber value $k_{cr} = \pi$ found by the linear stability analysis. The nonlinear stability

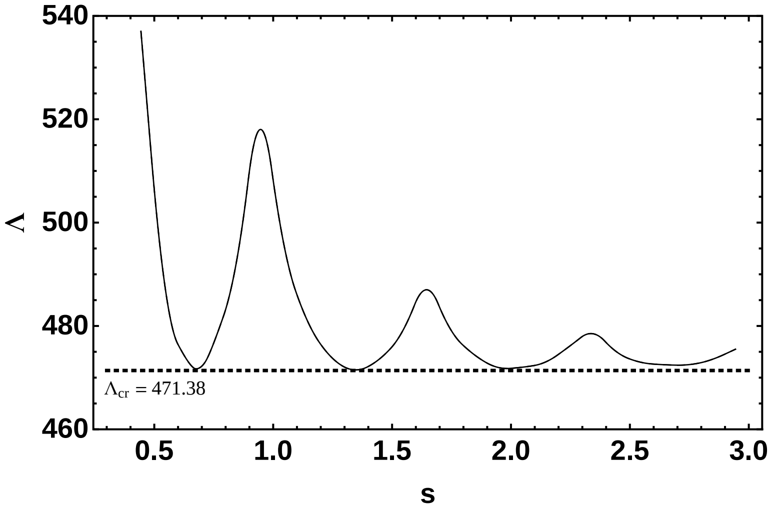

Figure 4. Critical values of Λ as a function of the aspect ratio s for a given value of the number of equations employed, $n = 90$, and two different values of the pair (Ge, R): $(Ge \to 0, R = 0)$, continuous line, and $(Ge = 1, R = 0)$, dashed line

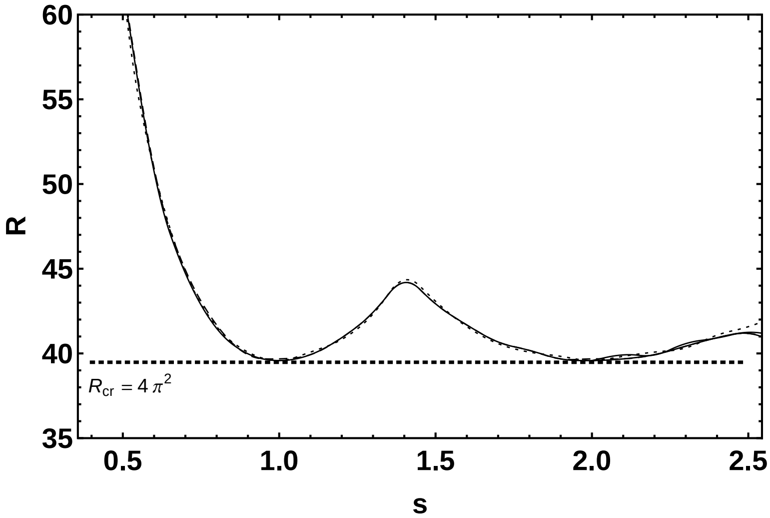

Figure 5. Critical values of R as a function of the aspect ratio s for $Ge \to 0$, $\Lambda = 10^{-4}$ and different values of the number of equations employed n

analysis here proposed is preliminary investigation of the problem presented. A partial investigation of the parametric range is indeed presented. Nonetheless it is a fairly good starting point for the investigation of nonlinear thermal instabilities. We may conclude that, in the parametric range here studied, the setup investigated does not present subcritical instabilities and the nonlinear stability analysis does not highlight a change behaviour with respect to the linear analysis.

References

Nield, D. A., Bejan, A. (2013), Convection in Porous Media, 4^{th} edition. Springer, New York.

Nield, D.A., (2007), The modeling of viscous dissipation in a saturated porous medium. *ASME Journal of Heat Transfer*, **129**, 1459–1463.

Storesletten, L., Barletta, A., (2009), Linear instability of mixed convection of cold water in a porous layer induced by viscous dissipation. *International Journal of Thermal Sciences*, **48**, 655–664.

Barletta, A., Celli, M., Rees, D. A. R. (2009), Darcy-Forchheimer flow with viscous dissipation in a horizontal porous layer: onset of convective instabilities. Stability analysis of natural convection in porous cavities through

Nield, D. A., Barletta, A., (2010), Extended Oberbeck-Boussinesq approximation study of convective instabilities in a porous layer with horizontal flow and bottom heating. *International Journal of Heat and Mass Transfer*, **53**, 577–585.

Cotta, R. M., (1998), The integral transform method in thermal & fluids sciences & engineering. Begell House, New York.

Pontes, J., de B. Alves, L. S., Cotta, R. M., (2002), Stability analysis of natural convection in porous cavities through integral transforms. *International Journal of Heat and Mass Transfer*, **45**, 1185–1195.